# Antimicrobial 14-Helical β-Peptides: Potent Bilayer Disrupting Agents†

Raquel F. Epand,‡ Tami L. Raguse,§ Samuel H. Gellman,§ and Richard M. Epand*,‡

*Department of Biochemistry, McMaster University Health Sciences Centre, Hamilton, ON, L8N 3Z5 Canada, and Department of Chemistry, University of Wisconsin, Madison, Wisconsin 53706*

*Received March 25, 2004; Revised Manuscript Received May 17, 2004*

ABSTRACT: The interactions of two amphiphilic and cationic, nine-residue β-peptides with liposomal membranes were studied. These β-peptides are shown to form 14-helices in the presence of bilayers. Membrane binding and membrane permeabilization occur preferentially in the presence of anionic lipids. The β-peptides have the ability to cause tranbilayer diffusion of phospholipids, form pores, and promote lipid mixing between liposomes. These β-peptides have previously been shown to display antimicrobial activity comparable to that of a longer β-peptide, β-17, which adopts a different type of helical conformation (12-helix), and to the 23 amino acid (Ala$^{8,13,18}$)-magainin-II-amide, which adopts an α-helical conformation. In addition, these 14-helical β-peptides show relatively low hemolytic activity. The biological potency and microbial specificity of the 14-helical β-peptides, despite their relatively short length, suggests that 14-helices can be particularly disruptive to microbial membranes.

Helix-forming antimicrobial peptides are critical components of the innate immune system, and these host-defense peptides are potential sources of new antibiotic drugs (*1*, *2*). Recently there has been growing interest in unnatural oligomers that mimic host-defense peptides (*3*, *4*), because unnatural oligomers are not subject to proteolytic degradation, in contrast to peptides composed of proteinogenic residues (*5*). Several groups have examined oligomers of β-amino acids ("β-peptides") in this context (*6*). These designs have been based on two different types of β-peptide helix, the 12-helix, containing 12-membered ring C═O(i)- -H−N(i+3) hydrogen bonds, and the 14-helix, containing 14-membered ring C═O(i)- -H−N(i-2) hydrogen bonds. For each of these β-peptide secondary structures, sequences that result in formation of an amphiphilic helix, with lipophilic groups aligned on one side and cationic groups on the other, display significant antimicrobial activity against a range of species (*7*−*12*).

We have recently characterized the interactions of a 12-helical β-peptide antibiotic with synthetic lipid vesicles (*13*), and here we report analogous studies with a pair of 14-helical β-peptide antibiotics, **1** and **2**. Compound **1** is closely related to a design originally developed by DeGrado et al. (*7*). The 14-helix has ca. three residues per turn (*6*); therefore, when β-peptides **1** or **2** adopt a 14-helical conformation, the helix has hydrophobic side chains on two-thirds of the helical circumference and cationic side chains on the other third. Most of the residues in β-peptides **1** and **2** are derived from β-substituted β-amino acids ("$\beta^3$-residues"). Previous work has shown that oligomers composed exclusively of $\beta^3$-residues adopt 14-helical conformations in organic solvents (e.g., methanol), but usually not in water (*6*). Three of the hydrophobic residues in β-peptide **2** are derived from *trans*-2-aminocyclohexanecarboxylic acid (*14*, *15*). This residue is a strong promoter of 14-helicity, even in aqueous solution (*16*, *17*). Circular dichroism (CD)[1] data reported by DeGrado et al. for β-peptides related to β-peptide **1** indicate that these molecules do not form the 14-helix in water but that 14-helicity can be induced by addition of micelles (*7*, *9*). β-Peptide **1** itself also shows no sign of 14-helicity in aqueous solution, but addition of 2,2,2-trifluoroethanol (TFE) induces partial 14-helix formation (*12*). In contrast, β-peptide **2** shows partial 14-helicity even in the absence of TFE (i.e., pure aqueous solution) (*12*).

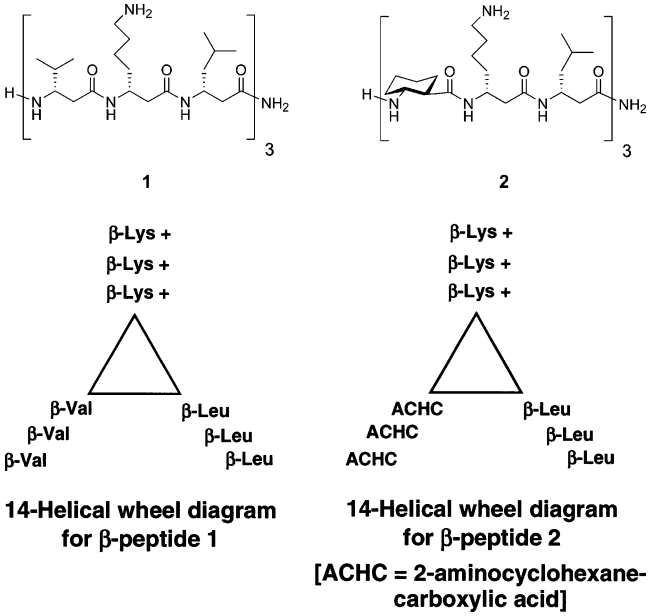


Both β-peptides **1** and **2** display significant bacteriostatic and bactericidal activity against four different microbial

† This work was supported by grant MT-7654 from the Canadian Institutes of Health Research and grant GM-56414 from the US National Institutes of Health. T.L.R. was supported in part by a pre-doctoral fellowship from the US National Science Foundation.

* To whom correspondence should be addressed. Tel.: (905) 525-9140. Fax: (905) 521-1397. E-mail: epand@mcmaster.ca.

‡ McMaster University Health Sciences Centre.

§ University of Wisconsin.

10.1021/bi049414l CCC: $27.50 
Published on Web 07/03/2004

species, and both can lyse bacterial cells (*12*). However, neither **1** nor **2** shows much tendency to lyse human red blood cells. This selectivity toward prokaryotic, relative to eukaryotic cell membranes, is commonly observed for natural host-defense peptides and may be the source of selectivity for prokaryotic cells in toxic effects (*1*). Interestingly, despite the significant difference in intrinsic helical stability between $\beta$-peptides **1** and **2**, the antimicrobial and hemolytic activities of these two $\beta$-peptides are quite similar (*12*).

In this study, we describe the interaction of $\beta$-peptides **1** and **2** with model membranes. We have studied changes in $\beta$-peptide conformation in the presence of lipid vesicles of varying composition. In addition, we have examined the effects of the $\beta$-peptides on liposome properties including membrane barrier integrity, lipid mixing, transbilayer diffusion, and lipid phase transitions. The lipids we have used in the present studies are shown below.

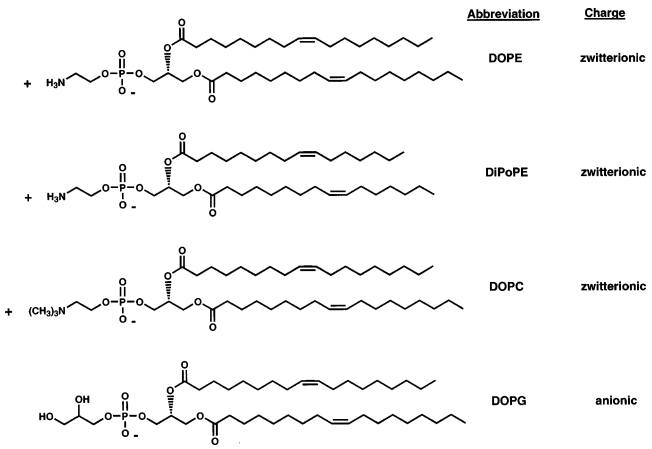


Phosphatidylcholine (PC) is zwitterionic and is a major lipid component of eukaryotic membranes. It is used in this work as a simple model for these plasma membranes; phosphatidylglycerol (PG) is anionic and is a major lipid component of prokaryotic cell membranes. We compare the interaction of the $\beta$-peptides with zwitterionic and anionic model membranes. In addition, we wish to assess the role of intrinsic membrane curvature in the interaction of these $\beta$-peptides with membranes. This is done both by measuring the effects of the peptide on the temperature of conversion of DiPoPE from the lamellar to the hexagonal phase as well as by substituting DOPE for DOPC to measure the effect of increased negative curvature strain on the modulation of lipid properties by these $\beta$-peptides. Finally, we assess membrane fusion using the mixture DOPE/DOPC/cholesterol (1:1:1). Liposomes composed of this zwitterionic lipid mixture are suitable to study membrane fusion because they are more prone to undergo fusion than simpler lipid mixtures, thus allowing for comparative studies to be made.

## MATERIALS AND METHODS

**Materials.** Phospholipids, including the fluorescently labeled lipids *N*−(lissamine Rhodamine B sulfonyl) phosphatidylethanolamine, *N*−(7-nitro-2,1,3-benzoxadiazol-4-yl) phosphatidylethanolamine, and 1-lauroyl-2-(1′-pyrenebutyroyl)-*sn*-glycero-3-phosphocholine (py-12-PC) were purchased from Avanti Polar Lipids (Alabaster, AL). The labeled lipids were made by chemical modification of phosphatidylethanolamine that was prepared from egg phosphatidylcholine by transphosphatidylation.

**Preparation of 1 and 2.** The synthesis and purification of these compounds have been described in detail (*12*).

**Preparation of Large Unilamellar Vesicles (LUVs).** Lipid films were made by dissolving appropriate amounts of lipid in a mixture of chloroform/methanol, 2/1 (v/v), followed by solvent evaporation under nitrogen to deposit the lipid as a film on the wall of a test tube. Final traces of solvent were removed in a vacuum chamber attached to a liquid nitrogen trap, for 2−3 h. Dried films were kept under Argon gas at −30 °C if not used immediately. Films were hydrated with buffer, vortexed extensively at room temperature, and then subjected to five cycles of freezing and thawing. The homogeneous lipid suspensions were then further processed by 10 passes through two stacked 0.1-$\mu$m polycarbonate filters (Nucleopore Filtration Products, Pleasanton, CA) in a high-pressure barrel extruder (Lipex Biomembranes, Vancouver, BC), at room temperature. LUVs were kept on ice and used within a few hours of preparation. Lipid phosphorus was determined by the method of Ames (*18*).

**Membrane Binding.** Binding studies were carried out by titrating a fixed amount of $\beta$-peptide solution in buffer composed of 10 mM HEPES, 0.14 M NaCl, and 1 mM EDTA, pH 7.4, with increasing amounts of lipid mixtures in the form of MLVs prepared by vortexing lipid films extensively with buffer. After 3 cycles of freezing and thawing, the mixtures were incubated at 37 °C for 1 h and then centrifuged at 190000 g for 180 min at 25 °C. The supernatant was collected, and the $\beta$-peptides were quantified with the CBQCA reagent (Molecular Probes), against a standard curve constructed for each of the $\beta$-peptides. Fluorescence was read in a 96-well plate with a SPECTRAmax Gemini XS Microplate Reader equipped with the software SOFTmax PRO v 3.1.2. Excitation was set at 485 nm and emission at 530 nm, with a cut off filter at 515 nm in the emission path. Analysis of the binding curves was done according to the method previously described (*19*, *20*).

**Circular Dichroism (CD).** The CD spectra were recorded using an AVIV Model 215 Circular Dichroism Spectrometer (Proterion Corp, Piscataway, NJ). The sample was contained in a 1-mm path length quartz cell that was maintained at 25 °C in a thermostated cell holder. The CD data are expressed as the mean residue ellipticity. All CD measurements were made with $\beta$-peptide dissolved in 10 mM sodium phosphate buffer containing 0.14 M NaF and 1 mM EDTA at pH 7.4. For samples containing lipid, the lipid was first made into a dry film from a solution of chloroform/methanol and was hydrated by vortexing with buffer. The lipid suspension was then sonicated to clarity to make SUVs.

[1] Abbreviations: $T_H$, bilayer to hexagonal transition temperature; DiPoPE, dipalmitoleoyl-phosphatidylethanolamine; CD, circular dichroism; DSC, differential scanning calorimetry; SUVs, small or sonicated unilamellar vesicles; MLVs, multilamellar vesicles; LUVs, large unilamellar vesicles; DOPC, dioleoylphosphatidylcholine; DOPE, dioleoylphosphatidylethanolamine; DOPG, dioleoylphosphatidylglycerol; N−Rh−PE, N−(lissamine Rhodamine B sulfonyl) phosphatidylethanolamine; N−NBD−PE, N−(7-nitro-2,1,3-benzoxadiazol-4-yl) phosphatidylethanolamine; ANTS, 8-aminonaphthalene-1,3,6-trisulfonic acid; DPX, *p*-xylene-bis-pyridinium bromide; L/P, lipid to peptide molar ratio; MIC, minimal inhibitory concentration; py-12-PC, 1-lauroyl-2-(1′-pyrenebutyroyl)-*sn*-glycero-3-phosphocholine; py-12-PS, 1-lauroyl-2-(1′-pyrenebutyroyl)-*sn*-glycero-3-phosphoserine; TFA, trifluoroacetic acid; TFE, trifluoroethanol.

**DSC.** Lipid films were prepared from DiPoPE dissolved in chloroform/methanol (2:1, v/v). Increasing mol fractions of β-peptides dissolved in methanol were added to the solution of lipid, and the solvent was removed by evaporation with nitrogen. Final traces of organic solvent were removed in a vacuum chamber attached to a liquid nitrogen trap for 2−3 h. The lipid films were hydrated at room temperature by vortexing with 20 mM Pipes buffer containing 0.14 M NaCl, 1 mM EDTA, and 0.002% sodium azide, pH 7.4. The final lipid concentration was 5 mg/mL. Lipid suspensions and buffer were degassed under vacuum before being loaded into the sample or the reference cell, respectively, of a NanoCal high sensitivity calorimeter (CSC, American Forks, UT). A heating scan rate of 0.75° K/min was employed. The observed phase transition was fitted with parameters describing an equilibrium with a single van't Hoff enthalpy and the transition temperature reported as that for the fitted curve. For some curves, two components were included in the fit of the data. The fit of the transition provides a measure of the average effect of the β-peptide on the curvature properties of the lipid. Data were analyzed with the program Origin 5.0.

**Leakage Studies with ANTS/DPX.** Leakage of aqueous contents from liposomes was determined using the ANTS-DPX assay (*21*). Lipid films were hydrated with 12.5 mM ANTS, 45 mM DPX, 68 mM NaCl, 10 mM Hepes, at pH 7.4. The osmolarity of this solution was adjusted to be equal to that of the buffer as measured with a cryoosmometer (Advanced Model 3MOplus Micro-Osmometer, Advanced Instruments Inc., Norwood, MA). LUVs of 0.1-μm diameter were prepared by extrusion as described above. After passage through a 2.5 × 20-cm column of Sephadex G-75, the void volume fractions were collected, and the phospholipid concentration was determined by phosphate analysis. The fluorescence measurements were performed in 2 mL of the buffer 10 mM Hepes, 0.14 M NaCl, 1 mM EDTA in a quartz cuvette equilibrated at 37 °C with stirring. Aliquots of LUVs were added to the cuvette to a final lipid concentration of 50 μM, and the fluorescence was recorded as a function of time with an SLM Aminco Bowman Series ll spectrofluorimeter, using an excitation wavelength of 360 nm and an emission wavelength of 530 nm with 8 nm bandwidth slits. A 490 nm cutoff filter was placed in the emission path. Leakage was initiated by addition of the β-peptide in buffer solution. The value for 100% leakage was obtained by adding 20 μL of a 10% Triton X-100 solution to the cuvette. Measurements were performed in duplicate.

**Lipid Mixing Assay.** The resonance energy transfer assay of Struck et al. (*22*) was used to monitor membrane fusion induced by the β-peptides. For each system, two populations of LUVs were prepared, one unlabeled and one labeled with 2 mol % each of N−Rh−PE and N−NBD-PE. A 9:1 molar ratio of unlabeled to labeled liposomes was used in the assay. Fluorescence was recorded in an SLM Aminco Bowman Series II spectrofluorimeter. The excitation and emission wavelengths were set at 465 and 530 nm, respectively, using a 490-nm cut off filter between the cuvette and the emission monochromator, with slits set for 8 nm bandwidths. Siliconized glass cuvettes (1-cm path length) were used with continuous stirring in a thermostated cuvette holder. Measurements were carried out at 37 °C in 10 mM HEPES, 140 mM NaCl, 1 mM EDTA buffer, pH 7.4. A freshly prepared solution of the β-peptide in buffer was added to 2 mL of 50 μM LUVs of DOPC/DOPE/cholesterol (1:1:1) buffer in the cuvette. Fluorescence was recorded for several minutes and then 20 μL of 10% Triton X-100 was added (final concentration 0.1%) to obtain the maximum fluorescence intensity value, $F_{max}$. The initial fluorescence intensity prior to addition of β-peptide, $F_0$, was taken as zero. Percent lipid mixing at time $t$ is given by: $((F_t - F_0)/(F_{max} - F_o))100$. Measurements were performed in duplicate and gave similar results.

**Rate of Lipid Transbilayer Diffusion.** The rate of transbilayer lipid diffusion (flip-flop) was measured using a method described by Müller et al. (*23*). The method is based on the dilution of a pyrene-labeled lipid probe as a result of transbilayer diffusion, causing a reduction in pyrene excimer emission. The probe stock was made by dissolving the pyrene-labeled lipid in ethanol and then adding it to PBS (pH 7.2) to a final ethanol concentration of 5 vol % (v/v). An aliquot of this stock solution of probe was then added to a suspension of 10 μM LUV in PBS pH 7.2, in a quartz cuvette, so that the probe partitioned into the outer monolayer at a concentration of 10 mol %, or 5 mol % of the total lipid. The ratio of the emission peaks for excimer and monomer fluorescence of pyrene was recorded as a function of time at 37 °C. An excitation wavelength of 344 nm was used with slits set for 4 nm bandwidths. The fluorescence of the monomeric form of the probe was measured at an emission wavelength of 395 nm and that of the excimer at 477 nm. Controls without the addition of β-peptide showed no change in fluorescence emission over time, indicating a very low basal rate of flip-flop. A positive control with magainin II was also run and gave very similar results to those previously reported (*23*). When flip-flop occurs, there is a reduction in the excimer-to-monomer ratio because of the dilution of the probe from one monolayer into both monolayers of the bilayer. Controls for effects on the fluorescence that were independent of flip-flop were conducted using symmetrically labeled LUVs. These symmetrically labeled LUVs were prepared by extrusion as described above, with the pyrene-labeled lipids mixed with the other lipids in organic solvent prior to generating the lipid film and hydrating.

## RESULTS

The partitioning of the two β-peptides between aqueous and membrane environments was measured using MLVs of different lipid compositions. The strongest partitioning to the membrane was found with anionic vesicles, DOPC/DOPG (1:2) for both β-peptides, with somewhat less partitioning into DOPE/DOPG (1:2) (Figure 1). There was no detectable binding of β-peptide **1** to DOPC bilayers, which are zwitterionic. In contrast, β-peptide **2** bound to pure DOPC membranes, but the characteristics of this binding were different from that with anionic membranes (i.e., those containing DOPG), with relatively little effect of increasing lipid concentration on the fraction of peptide bound.

The CD spectra of the β-peptides were measured at 25 °C (Figure 2) in the presence of mixtures of DOPC/DOPG (1:2) (top panel) DOPE/DOPG (1:2) (middle panel) or DOPC alone (bottom panel). These lipid systems were chosen to evaluate the role of anionic lipids (DOPG) and the influence

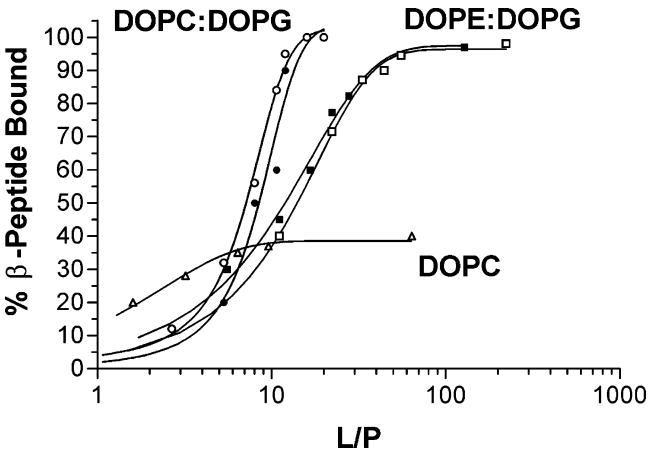


FIGURE 1: Partitioning of $\beta$-peptides between membrane and aqueous phases, as a function of lipid-to-peptide ratio. $\beta$-Peptide concentration was 25 $\mu$M. $\beta$-Peptide **1** in DOPC/DOPG (2:1) (●); $\beta$-peptide **1** in DOPE/DOPG (2:1) (■); $\beta$-peptide **2** in DOPC/DOPG (2:1) (○); $\beta$-peptide **2** in DOPE/DOPG (2:1) (□); $\beta$-peptide **2** in DOPC (△). Curves were generated by fitting the data points to a Boltzman sigmoidal function with strict criteria for convergence.

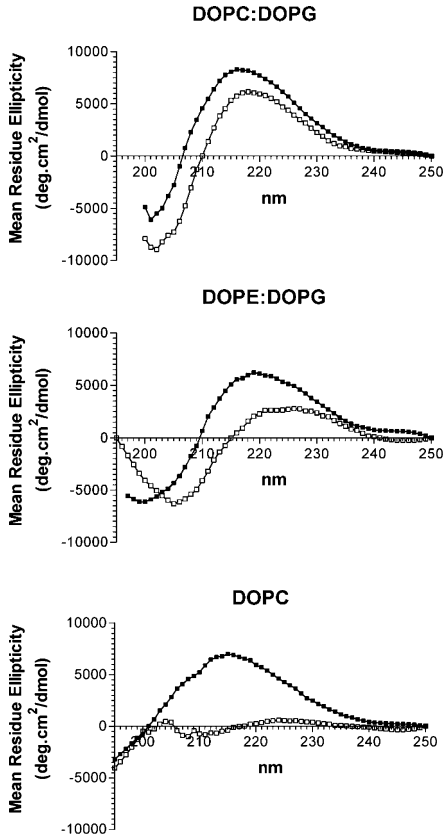


FIGURE 2: Circular dichroism spectra of $\beta$-peptide **1** (□) and $\beta$-peptide **2** (■) in the presence of SUVs. Top panel, DOPC/DOPG (1:2); middle panel, DOPE/DOPG (1:2); bottom panel, DOPC. All spectra are measured at 25 °C with 100 $\mu$M $\beta$-peptide. L/P = 5.

of a lipid such as DOPE with a high tendency (relative to that of DOPC) toward forming nonlamellar phases. Measurements were performed at a lipid to $\beta$-peptide ratio (L/P) of 5:1. Solutions of $\beta$-peptide **1** in DOPC did not exhibit significant ellipticity in the far UV CD spectrum, which matches previously reported far-UV CD data for $\beta$-peptide **1** in pH 7.2 aqueous buffer (*12*) and suggests a lack of 14-helix induction in $\beta$-peptide **1** by zwitterionic membranes. Figure 2 (bottom panel) shows that rigidified $\beta$-peptide **2** displays a maximum at ca. 215 nm and a zero-crossing at ca. 200 nm in the presence of DOPC vesicles. This CD spectrum is very similar to that displayed by $\beta$-peptide **2** in the absence of DOPC vesicles (*12*) and reflects partial 14-helix formation.

In contrast to zwitterionic DOPC vesicles, which exerted no effect on the CD spectrum of flexible $\beta$-peptide **1**, anionic vesicles containing DOPG significantly altered the CD spectrum of this $\beta$-peptide (Figure 2, top and middle panels). Lipid systems composed of DOPC/DOPG and DOPE/DOPG induced partial 14-helicity in $\beta$-peptide **1**, as indicated by maxima at ca. 218 nm and ca, 225 nm, respectively. The effect of DOPG-containing vesicles on rigidified $\beta$-peptide **2** was more subtle: the mixed vesicles caused the maximum and zero-crossing to shift to higher wavelengths relative to pure DOPC vesicles or aqueous buffer. This shift may indicate that binding to the vesicle surface causes a slight change in the 14-helix geometry. A similar hypothesis could explain the difference between the CD spectra of $\beta$-peptide **1** in the presence of DOPE/DOPG versus DOPC/DOPG vesicles. It is interesting that neither type of DOPG-containing vesicle seemed to cause a significant increase in the 14-helicity of $\beta$-peptide **2**, relative to aqueous buffer alone, as judged by mean residue ellipticity at the maximum.

It has previously been reported that dodecyl phosphocholine micelles induce 14-helix formation in $\beta$-peptides related to $\beta$-peptide **1** (composed entirely of acyclic residues) that, like $\beta$-peptide **1**, do not form the 14-helix in aqueous buffer (*7*, *9*). This helix-inducing effect of a zwitterionic detergent stands in contrast to our observation that zwitterionic vesicles do not induce 14-helix formation in $\beta$-peptide **1**, and that vesicles with a negative charge are required for helical folding of $\beta$-peptide **1**. The contrast suggests that detergent micelles are imperfect models for lipid bilayers.

DSC was used to measure the effect of the $\beta$-peptides on the lamellar to hexagonal phase transition of DiPoPE. This lipid converts from the bilayer to the hexagonal phase at 43 °C. The shift in the bilayer to hexagonal phase transition temperature ($T_H$) upon addition of $\beta$-peptide indicates how the $\beta$-peptide modulates the tendency toward formation of nonbilayer structures, and therefore, provides a measure of the effect of the $\beta$-peptide on the monolayer curvature propensities of the membrane. For these experiments, small amounts of $\beta$-peptide are added to the lipid to determine how the $\beta$-peptide, as an additive to the membrane, will affect membrane curvature. We express the amount of $\beta$-peptide added in terms of its mol fraction, as has been done with other systems (*13*). $\beta$-Peptides **1** and **2** exhibit nonmonotonic behavior, as a function of peptide-to-lipid ratio, in their effects on $T_H$ (Figure 3). At very low concentrations in the bilayer, both $\beta$-peptides lower $T_H$. This is a characteristic of a fusogenic peptide (*24*). At higher $\beta$-peptide concentrations, this effect is reversed. This behavior is not unique to these $\beta$-peptides; similar behavior has been reported for the fusion peptide of feline leukemia virus (*25*). A possible explanation for this nonmonotonic behavior is that the $\beta$-peptide aggregates in the membrane at higher concentrations, and the aggregate has different effects on membrane curvature from the monomeric $\beta$-peptide. A further complexity was observed for $\beta$-peptide **2**: at higher $\beta$-peptide concentrations, the bilayer to hexagonal phase transition of DiPoPE is split into

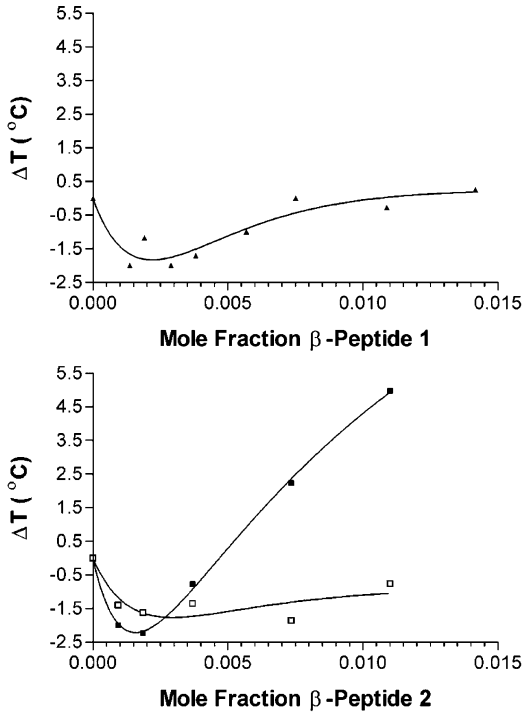


FIGURE 3: Peptide-induced shifts in the bilayer to hexagonal transition temperature of DiPoPE ($\Delta T$) as a function of the mol fraction of peptide. $T_H$ was measured with DSC using heating scans at 0.75 °C/min. Top curve, $\beta$-peptide **1**; Bottom curve, $\beta$-peptide **2**. The graph for $\beta$-peptide **2** shows the temperature of each of the two components of the transition. Data points were fitted to a two-site binding hyperbola with strict criteria for convergence.

two components, as seen in the DSC scans (not shown). Deconvolution of the experimental data indicated that one component has a lower $T_H$ than the pure lipid, and the other component has a higher $T_H$ than the pure lipid. The former component may be caused by the $\beta$-peptide monomer, which may have a limited solubility in the membrane, while the latter component may represent domains containing aggregates of $\beta$-peptide **2**.

Leakage of aqueous contents was analyzed using LUVs. The LUV lipid compositions were different from that used in the DSC to assess effects of the peptides on membrane curvature. It is not intended that the magnitudes of the shifts in $T_H$ should be compared with the extent of membrane leakage. In the case of leakage, the results are given for different lipid-to-peptide ratios (L/P) on the right-hand side of each curve. $\beta$-Peptide **1** causes the largest amount of leakage of ANTS from LUVs of DOPC:DOPG (1:2) relative to other lipids (Figure 4A). Substitution of DOPE for DOPC greatly reduces the amount of ANTS leakage (Figure 4B), while ANTS leakage from pure DOPC vesicles (Figure 4C) is very low. In the case of $\beta$-peptide **2**, there is rapid leakage of ANTS from LUVs containing DOPG mixed with either DOPC (Figure 5A) or DOPE (Figure 5B), while the ANTS leakage from pure DOPC vesicles is lower (Figure 5C).

$\beta$-peptides **1** and **2** showed significant fusogenic activity, independent of the presence of anionic lipid headgroups, as indicated by their ability to promote the mixing of lipids present initially in distinct vesicle populations. However, $\beta$-peptide **2** exhibited a nonmonotonic effect on lipid mixing, with mixing increasing dramatically as lipid to $\beta$-peptide ratio rose to 10:1 and then decreasing markedly as the lipid to

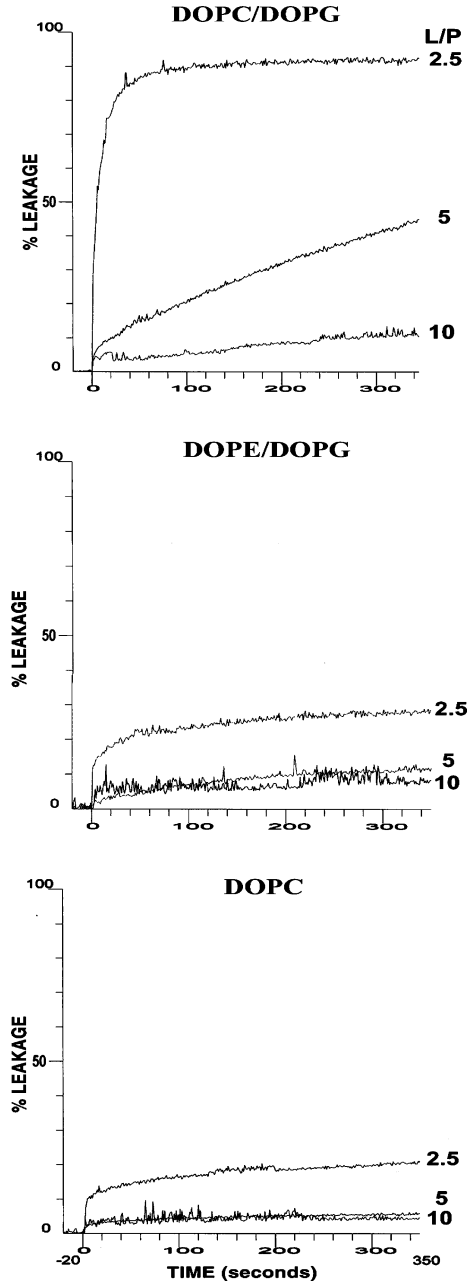


FIGURE 4: Time dependence of vesicle leakage of the small fluorophore ANTS promoted by $\beta$-peptide **1** using 50 $\mu$M LUVs of (A) DOPC/DOPG (1:2), (B) DOPE/DOPG (1:2) and (C) DOPC. Measurements were made at 37 °C. L/P is 2.5:1, 5:1, or 10:1 and is indicated on the right-hand side of each curve.

$\beta$-peptide ratio continued to rise (Figure 6). This nonmonotonic effect was not observed with $\beta$-peptide **1** and could be the result of the peptide aggregation in the membrane. It is known that lipid mixing is more rapid in systems with increasing negative curvature strain. The biphasic behavior of peptide **2** in membrane fusion (Figure 6, part 2), is anticipated from the biphasic effects of this peptide on membrane curvature (Figure 3).

Leakage and fusion are both manifestations of membrane destabilization. Although leakage can proceed independently of fusion, most fusion processes in liposomes are leaky. Both leakage and fusion are induced rapidly by $\beta$-peptides **1** and **2**.

A rapid rate of lipid transbilayer movement ("flip-flop") of py-12-PC is induced by $\beta$-peptides **1** and **2** (Figure 7).

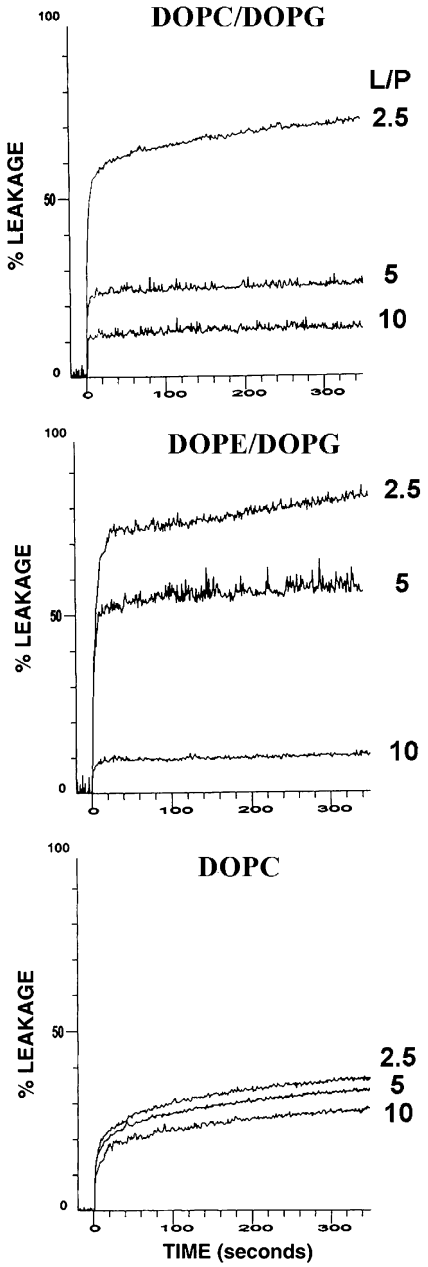


FIGURE 5: Time dependence of vesicle leakage of the small fluorophore ANTS promoted by $\beta$-peptide **2** using 50 $\mu$M LUVs of (A) DOPC/DOPG (1:2), (B) DOPE/DOPG (1:2), and (C) DOPC. Measurements were made at 37 °C. L/P is 2.5:1, 5:1, or 10:1 and is indicated on the right-hand side of each curve.

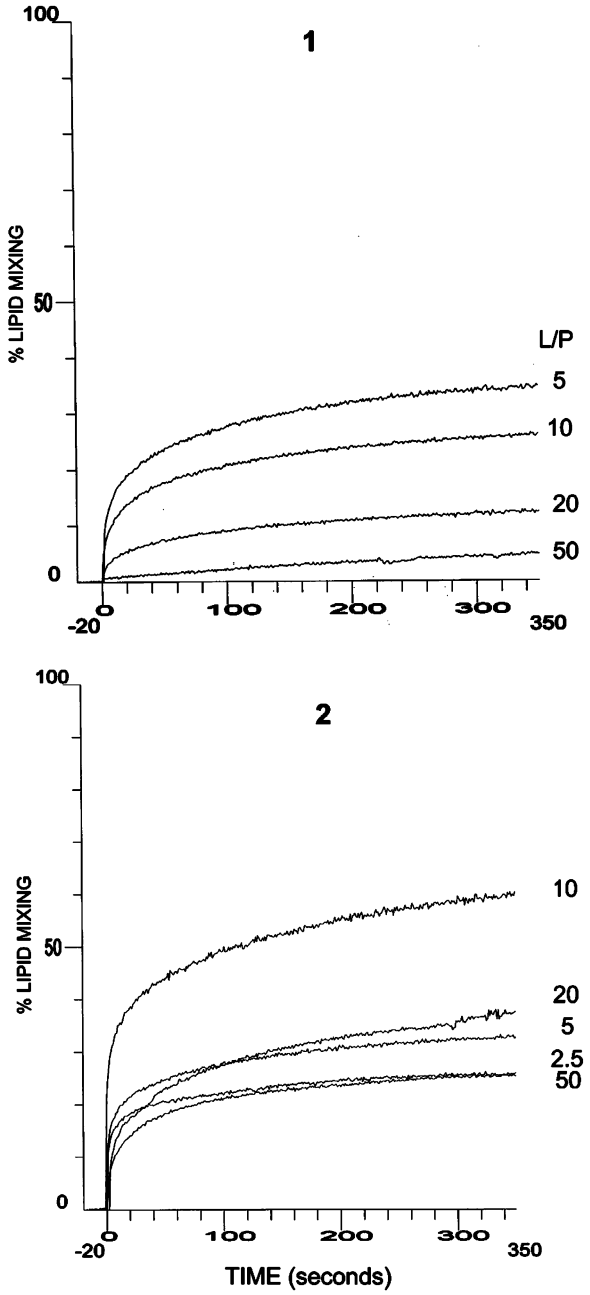


FIGURE 6: Time dependence of lipid mixing promoted by $\beta$-peptide **1** (top) or by $\beta$-peptide **2** (bottom) using 50 $\mu$M LUVs of DOPC/DOPE/cholesterol (1:1:1). Measurements made at 37 °C. L/P is indicated on the right-hand side of each curve.

The rate of flip-flop of py-12-PC is very slow in the absence of $\beta$-peptide. Control experiments showed that the decrease in excimer/monomer ratio of py-12-PC caused by the $\beta$-peptides arises from lipid dilution via flip-flop rather than from some other effect: neither **1** nor **2** influenced the emission ratio observed for vesicles prepared with a symmetrical distribution of the probe lipid ("Sym"). In the Sym vesicles, each of the two monolayers has the same mol fraction of py-12-PC as is present in only the outer monolayer of the test vesicles. Thus, the initial Ie/Im ratio of the Sym liposomes should be the same as that of the test vesicles. Any decrease in this ratio caused by the $\beta$-peptide would indicate that Ie/Im changes arise from a mechanism other than flip-flop. The Sym data in Figure 7 show that no alternative mechanism is operative in the present studies.

## DISCUSSION

The results reported here allow us to compare the properties of $\beta$-peptides **1** and **2** with those of a different $\beta$-peptide, $\beta$-17 (*8*, *11*, *13*), and those of (Ala$^{8,13,18}$)-magainin-II-amide (*26*), a synthetic analogue of the naturally occurring host-defense peptide magainin-II, with sequence: GIGK-FLHAAKKFAKAFVAEAMNS-amide. Antimicrobial $\beta$-peptides and engineered variants of natural antimicrobial peptides are of interest because of their potential clinical use against pathogens that are resistant to conventional antibiotics.

$\beta$-Peptides **1**, **2**, $\beta$-17 and (Ala$^{8,13,18}$)-magainin-II-amide all exhibit minimum inhibitory concentrations (MIC) against a number of bacteria that are almost two orders of magnitude lower than the concentration required to induce hemolysis

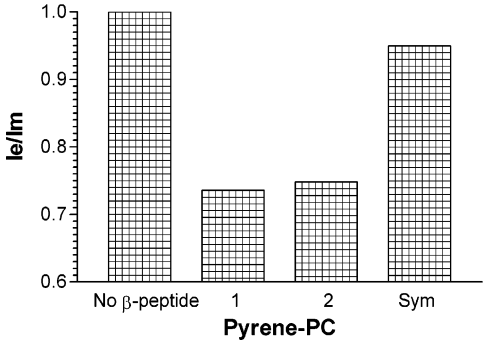


FIGURE 7: Rate of transbilayer diffusion of py-12-PC. A decrease in the ratio of Ie (intensity of excimer emission) to Im (intensity of monomer emission) reflects transbilayer diffusion. The extent of this translocation is measured over 200 s and is negligible for LUVs in the absence of β-peptide (first bar). The concentration of liposomes of DOPC/DOPG (1:2) was 10 μM, and the L/P was 5. Symmetrically labeled control liposomes (labeled Sym) were also treated with β-peptides **1** or **2**, with the two β-peptides producing only small changes in the Ie/Im ratio, at 37 °C. Bars represent the average of two measurements within a single batch of vesicles and were reproducible to within 10%.

(*8*, *11*, *12*, *26*). The antimicrobial potencies of these four molecules are similar to one another against four different bacteria (the MIC values vary from bacterium to bacterium). All four are capable of adopting amphiphilic helical conformations, with positive charge localized on one side of the helix and lipophilic side chains localized on the other side. At neutral pH, β-peptides **1** and **2** should have a net charge of +4, β-17 should have a net charge of +6, and (Ala$^{8,13,18}$)-magainin-II-amide should have net charge of +4 to +5 (uncertainty arises because there is one His residue in this sequence). Most natural host-defense peptides are cationic. It is widely believed that net positive charge plays a role in generating selectivity toward bacteria rather than toward eukaryotic cells, since bacterial membranes carry larger net negative charge than does the outer monolayer of eukaryotic cells. Most anionic lipids in healthy eukaryotic cells reside in the inner leaflet of the cytoplasmic membrane.

Three distinct helical conformations are represented among (Ala$^{8,13,18}$)-magainin-II-amide and β-peptides **1**, **2** and β-17. The β-peptide 12-helix, formed by β-17, and the familiar α-helix, formed by (Ala$^{8,13,18}$)-magainin-II-amide, have similar overall geometries (*27*). In contrast, the β-peptide 14-helix is somewhat wider. For (Ala$^{8,13,18}$)-magainin-II-amide and β-peptide **1** helical folding must be induced by an anionic membrane surface, while for β-peptide **2** and β-17 helicity is observed in aqueous solution alone.

β-Peptides **1** and **2**, with 9 β-residues each, are significantly shorter than β-17 (17 β-residues) or (Ala$^{8,13,18}$)-magainin-II-amide (23 α-residues). β-17 in the 12-helical conformation is about the same length as (Ala$^{8,13,18}$)-magainin-II-amide in the α-helical conformation (ca. 35Å); β-peptides **1** and **2** in the 14-helical conformation are only about half this length (ca. 15 Å). In light of these length differences, it is surprising that short 14-helical β-peptides **1** and **2** display antimicrobial potency comparable to that of (Ala$^{8,13,18}$)-magainin-II-amide or β-17, particularly since we have found that 11-residue analogues of β-17 are considerably less potent than β-17 itself (Porter, E. A., Weisblum, B.; Gellman, S. H., manuscript in preparation). These comparisons raise the possibility that the 14-helix conformation is somehow particularly effective, relative to the α-helix or the 12-helix, at disrupting bacterial membranes.

The β-peptide **1** and its enantiomer display indistinguishable antibacterial activity, which suggests that these molecules do not kill bacteria by forming specific complexes with protein targets (*12*). β-Peptides **1** and **2** and (Ala$^{8,13,18}$)-magainin-II-amide, at 20 μg/mL, all cause leakage of β-galactosidase (MW > 100 kD) from *B. subtilis* cells. This behavior indicates that (Ala$^{8,13,18}$)-magainin-II-amide and β-peptides **1** and **2** are capable of causing large-scale membrane disruptions, at least under some conditions. β-Galactosidase leakage from *B. subtilis* is slightly more strongly promoted by (Ala$^{8,13,18}$)-magainin-II-amide than by β-peptides **1** and **2** (*12*), although in liposomes, magainin does not cause permeabilization of 21.2 kD dextrans (*28*). Thus, β-peptides **1** and **2** (Figures 4 and 5) and (Ala$^{8,13,18}$)-magainin-II-amide all are capable of forming pores in lipid bilayers. The extent of membrane disruption, however, seems to be dependent on the particular system used.

The pore mechanism of antimicrobial peptide action predicts that lipid flip-flop will be promoted by pore-forming peptides (*29*). Our results demonstrate that β-peptides **1** and **2** can induce lipid flip-flop in bilayers containing anionic lipids (Figure 7), which is consistent with the conclusion that these β-peptides can form pores in lipid bilayers. These large pores must involve the assembly of several β-peptide molecules. In addition, aggregation of these β-peptides alters effects on membrane curvature and decreases lipid mixing. Lipid mixing requires negative curvature that would be inhibited by β-peptide aggregation. In contrast, leakage by a pore mechanism requires positive curvature and would be facilitated by β-peptide assembly.

Effects of these peptides on membrane curvature were evaluated by measuring the shift in the $T_H$ of DiPoPE as a function of β-peptide concentration in the MLVs. β-Peptides **1** and **2** exhibit nonmonotonic behavior as a function of β-peptide mol fraction (Figure 3): both lower $T_H$ at low mol fractions of peptide, but $T_H$ rises at higher ones. As described above, β-peptide **1** does not bind to DOPC, a zwitterionic lipid, but it does affect the transition temperature of DiPoPE. Although phosphatidylethanolamine is largely zwitterionic, it carries a small negative charge at neutral pH because the amino group is not entirely protonated. This would facilitate the binding of **1**, although the membrane partitioning of this β-peptide may not be complete. The rise in $T_H$ at higher β-peptide mole fraction is particularly dramatic for **2**. In contrast, β-17 monotonically lowers $T_H$ (*13*) and (Ala$^{8,13,18}$)-magainin-II-amide monotonically raises $T_H$ with increasing mol fractions. The results with (Ala$^{8,13,18}$)-magainin-II-amide fit in well with the pore model of membrane leakage, which requires the peptide to induce positive curvature (*29*). The molecular mechanism of leakage induction by peptides that promote negative curvature has not been well described. When sufficiently large amounts of β-peptide **2** are present (Mol fractions > 0.005) there is promotion of positive curvature, as indicated by shifts in $T_H$ (Figure 3). We suggest that at higher peptide concentrations these liposomes are destabilized by promotion of positive curvature, that is, by a pore-forming mechanism similar to that of (Ala$^{8,13,18}$)-magainin-II-amide.

Both β-peptides **1** and **2** can cause membrane fusion (Figure 6). Fusion is often promoted by peptides that increase

negative bilayer curvature (*25*, *30*, *31*). The β-peptides in this study promote negative curvature at very low peptide concentrations (Figure 3). A possible relationship between membrane fusion and antimicrobial action has been suggested for some antimicrobial peptides that inhibit the growth of Gram negative bacteria, perhaps by inducing the fusion of the cell wall and cell membrane (*32*). However, for the two β-peptides studied in this work, MIC values against the Gram positive strains *S. aureus* and *E. faecium* are in the same range as that found against Gram negative bacterium *E. coli* (*33*). Therefore, membrane fusion-related activity cannot explain the antimicrobial activity of β-peptides **1** and **2** observed in Gram negative bacteria. Recently, it has been shown that, at sufficiently high concentrations, antimicrobial peptides can penetrate the lipopolysaccharide monolayer of the outer membrane of Gram-negative bacteria (*34*), and thus the inner bacterial membrane becomes accessible to these peptides.

There are many similarities in the mode of action of β-peptides **1** and **2** *vis a vis* model membranes. Both β-peptides form 14-helices in bilayers, both show nonmonotonic effects on bilayer curvature as a function of peptide-to-lipid ratio, both bind and permeabilize anionic bilayers in preference to zwitterionic bilayers, and both cause lipid mixing and lipid flip-flop. Lipid mixing, flip-flop, and permeabilization occur when liposomes are exposed to the β-peptides, and these processes could be promoted in bacterial membranes, which would explain why β-peptides **1** and **2** exhibit similar antimicrobial activity. Overall, the two β-peptides conform to the Shai-Matsuzaki-Huang (SMH) model (*2*), developed to explain the mode of action of cationic antimicrobial peptides, which proposes that the initial interaction of the peptide with the membrane is electrostatic and that the peptide binds at the membrane interface, resulting in a thinning of the membrane. When the peptide concentration is sufficiently high, the peptides associate and penetrate the membrane to form a pore that is lined with both lipid and peptide. The peptide is then able to enter the target cell, dissipating its concentration gradient across the membrane, closing the pore.

β-Peptides **1** and **2** differ in intrinsic helix-forming propensity: β-peptide **1**, built entirely from acyclic β-amino acid residues, does not adopt the 14-helical conformation in aqueous solution, but β-peptide **2**, containing some cyclic residues, forms significant 14-helicity under these conditions. Addition of lipid vesicles has relatively little effect on the 14-helicity of β-peptide **2**, but vesicles induce partial 14-helix formation in β-peptide **1**, if the vesicles contain anionic lipid (Figure 2). This difference in conformational propensity, coupled with the very similar net hydrophobicities of β-peptides **1** and **2**, as judged by reverse phase HPLC retention (*12*) and their similar antimicrobial activities, suggests that it is the conformation of the peptide when bound to an anionic membrane, not the conformation in solution, that plays a significant role in determining biological efficacy. The results presented above show that the difference in conformational stability between β-peptides **1** and **2** manifests itself in several aspects of their interactions with liposomes. For example, rigid β-peptide **2** binds to zwitterionic DOPC vesicles, albeit weakly, while flexible β-peptide **1** does not (Figure 1). Rigid β-peptide **2** shows two-component behavior in its effects on the hexagonal transition temperature of bilayers, while flexible β-peptide **1** does not. At low lipid-to-peptide ratios, β-peptide **2** causes extensive leakage from DOPE:DOPG vesicles (Figure 5), but β-peptide **1** does not (Figure 4). However, these and other differences between β-peptides **1** and **2** summarized in this manuscript do not appear to have a significant impact on antimicrobial activity.

The 14-helical β-peptides **1** and **2** have particularly potent antimicrobial activity for their length, relative to 12-helical β-peptides and α-helical α-peptides. The 14-helix is somewhat wider than either the 12-helix or the α-helix, and perhaps this geometric difference influences their antimicrobial activity. Their high potency may indicate that the 14-helix is a particularly good scaffold for creating microbial membrane-disrupting agents.

## ACKNOWLEDGMENT

We are grateful to J. Lai for providing helpful assistance.

## REFERENCES

1. Tossi, A., Sandri, L., and Giangaspero, A. (2000) Amphipathic, α-helical antimicrobial peptides, *Biopolymers 55*, 4−30.
2. Zasloff, M. (2002) Antimicrobial peptides of multicellular organisms, *Nature 415*, 389−395.
3. Patch, J. A., and Barron, A. E. (2002) Mimicry of bioactive peptides via nonnatural, sequence-specific peptidomimetic oligomers, *Curr. Opin. Chem. Biol. 6*, 872−877.
4. Tew, G. N., Liu, D., Chen, B., Doerksen, R. J., Kaplan, J., Carroll, P. J., Klein, M. L., and DeGrado, W. F. (2002) De novo design of biomimetic antimicrobial polymers, *Proc. Natl. Acad. Sci. U.S.A 99*, 5110−5114.
5. Seebach, D., Abele, S., Schreiber, J. V., Martinoni, B., Nussbaum, A. K., Schild, H., Schulz, H., Hennecke, H., Woessner, R., and Bitsch, F. (1998) Biological and pharmacokinetic studies with β-peptides, *Chimia 52*, 734−739.
6. Cheng, R. P., Gellman, S. H., and DeGrado, W. F. (2001) β-Peptides: from structure to function, *Chem. Rev. 101*, 3219−3232.
7. Hamuro, Y., Schneider, J. P., and DeGrado, W. F. (1999) De novo design of antibacterial β-peptides, *J. Am. Chem. Soc. 121*, 12200−12201.
8. Porter, E. A., Wang, X., Lee, H. S., Weisblum, B., and Gellman, S. H. (2000) Nonhaemolytic β-amino acid oligomers, *Nature 404*, 565.
9. Liu, D., and DeGrado, W. F. (2001) De Novo design, synthesis, and characterization of antimicrobial peptides, *J. Am. Chem. Soc. 123*, 7553−7559.
10. LePlae, P. R., Fisk, J. D., Porter, E. A., Weisblum, B., and Gellman, S. H. (2002) Tolerance of acyclic residues in the β-peptide 12-helix: access to diverse side-chain arrays for biological applications, *J. Am. Chem. Soc. 124*, 6820−6821.
11. Porter, E. A., Weisblum, B., and Gellman, S. H. (2002) Mimicry of host-defense peptides by unnatural oligomers: Antimicrobial β-peptides, *J. Am. Chem. Soc. 124*, 7324−7330.
12. Raguse, T. L., Porter, E. A., Weisblum, B., and Gellman, S. H. (2002) Structure−activity studies of 14-helical antimicrobial β-peptides: Probing the relationship between conformational stability and antimicrobial potency, *J. Am. Chem. Soc. 124*, 12774−12785.
13. Epand, R. F., Umezawa, N., Porter, E. A., Gellman, S. H., and Epand, R. M. (2003) Interactions of the antimicrobial β-peptide β-17 with phospholipid vesicles differ from membrane interactions of magainins, *Eur. J. Biochem. 270*, 1240−1248.
14. Berkessel, A., Glaubitz, K., and Lex, J. (2002) *J. Org. Chem. 17*, 2948.
15. Schinnerl, M., Murray, J. K., Langenhan, J. M., and Gellman, S. H. (2003) Asymmetric synthesis of a new helix-forming β-amino acid: *trans*-4-aminopiperidine-3-carboxylic acid, *Eur. J. Org. Chem.* 721−726.

16. Appella, D. H., Barchi, J. J., Durell, S. R., and Gellman, S. H. (1999) Formation of short, stable helices in aqueous solution by β-amino acid hexamers, *J. Am. Chem. Soc. 121*, 2309−2310.
17. Raguse, T. L., Lai, J. R., and Gellman, S. H. (2003) Environment-independent 14-helix formation in short β-peptides: striking a balance between shape control and functional diversity, *J Am. Chem. Soc. 125*, 5592−5593.
18. Ames, B. N. (1966) Assay of inorganic phosphate, total phosphate, and phosphatases., *Methods Enzymol. 8*, 115−118.
19. Peitzsch, R. M., and McLaughlin, S. (1993) Binding of acylated peptides and fatty acids to phospholipid vesicles: pertinence to myristoylated proteins, *Biochemistry 32*, 10436−10443.
20. Ben Tal, N., Honig, B., Miller, C., and McLaughlin, S. (1997) Electrostatic binding of proteins to membranes. Theoretical predictions and experimental results with charybdotoxin and phospholipid vesicles, *Biophys. J. 73*, 1717−1727.
21. Ellens, H., Bentz, J., and Szoka, F. C. (1985) $H^+$- and $Ca^{2+}$-induced fusion and destabilization of liposomes, *Biochemistry 24*, 3099−3106.
22. Struck, D. K., Hoekstra, D., and Pagano, R. E. (1981) Use of resonance energy transfer to monitor membrane fusion, *Biochemistry 20*, 4093−4099.
23. Muller, P., Schiller, S., Wieprecht, T., Dathe, M., and Herrmann, A. (2000) Continuous measurement of rapid transbilayer movement of a pyrene-labeled phospholipid analogue, *Chem. Phys. Lipids 106*, 89−99.
24. Epand, R. M. (2003) Fusion peptides and the mechanism of viral fusion, *Biochim. Biophys. Acta 1614*, 116−121.
25. Davies, S. M., Epand, R. F., Bradshaw, J. P., and Epand, R. M. (1998) Modulation of lipid polymorphism by the feline leukemia virus fusion peptide: implications for the fusion mechanism, *Biochemistry 37*, 5720−5729.
26. Chen, H. C., Brown, J. H., Morell, J. L., and Huang, C. M. (1988) Synthetic magainin analogues with improved antimicrobial activity, *FEBS Lett. 236*, 462−466.
27. Lee, H. S., Syud, F. A., Wang, X. F., and Gellman, S. H. (2001) Diversity in short β-peptide 12-helices: High-resolution structural analysis in aqueous solution of a hexamer containing sulfonylated pyrrolidine residues, *J. Am. Chem. Soc. 123*, 7721−7722.
28. Hara, T., Kodama, H., Kondo, M., Wakamatsu, K., Takeda, A., Tachi, T., and Matsuzaki, K. (2001) Effects of peptide dimerization on pore formation: Antiparallel disulfide-dimerized magainin 2 analogue, *Biopolymers 58*, 437−446.
29. Matsuzaki, K., Sugishita, K., Ishibe, N., Ueha, M., Nakata, S., Miyajima, K., and Epand, R. M. (1998) Relationship of membrane curvature to the formation of pores by magainin 2, *Biochemistry 37*, 11856−11863.
30. Epand, R. M., Epand, R. F., Martin, I., and Ruysschaert, J. M. (2001) Membrane interactions of mutated forms of the influenza fusion peptide, *Biochemistry 40*, 8800−8807.
31. Epand, R. M. (1998) Lipid polymorphism and protein−lipid interactions, *Biochim. Biophys. Acta 1376*, 353−368.
32. Oh, J. T., Cajal, Y., Skowronska, E. M., Belkin, S., Chen, J., Van Dyk, T. K., Sasser, M., and Jain, M. K. (2000) Cationic peptide antimicrobials induce selective transcription of micF and osmY in *Escherichia coli*, *Biochim. Biophys. Acta 1463*, 43−54.
33. Markin, V. S., Kozlov, M. M., and Borovjagin, V. L. (1984) On the theory of membrane fusion. The stalk mechanism, *Gen. Physiol. Biophys. 3*, 361−377.
34. Ding, L., Yang, L., Weiss, T. M., Waring, A. J., Lehrer, R. I., and Huang, H. W. (2003) Interaction of antimicrobial peptides with lipopolysaccharides, *Biochemistry 42*, 12251−12259.

BI049414L